



# MFAP2 induces epithelial-mesenchymal transformation of osteosarcoma cells by activating the Notch1 pathway

Shan Jiang<sup>#</sup>, Ziang Zheng<sup>#</sup>, Bo Yuan, Rushan Yan, Qijun Yao, Haoran Chen, Yongxun Zhang, Yue Lei, Haidong Liang<sup>^</sup>

Department of Bone and Soft Tissue Repair and Reconstructive Surgery, The Second Hospital of Dalian Medical University, Dalian, China

**Contributions:** (I) Conception and design: S Jiang, Z Zheng, H Liang; (II) Administrative support: B Yuan; (III) Provision of study materials or patients: B Yuan, Q Yao, H Chen; (IV) Collection and assembly of data: B Yuan, R Yan, Y Zhang; (V) Data analysis and interpretation: S Jiang, Z Zheng, R Yan, H Chen, Y Lei; (VI) Manuscript writing: All authors; (VII) Final approval of manuscript: All authors.

<sup>#</sup>These authors contributed equally to this work as co-first authors.

**Correspondence to:** Haidong Liang, MD. Department of Bone and Soft Tissue Repair and Reconstructive Surgery, The Second Hospital of Dalian Medical University, No. 467, Zhongshan Road, Shahekou District, Dalian 116000, China. Email: johnhddmu@outlook.com.

**Background:** Osteosarcoma (OS) is a malignancy originating from mesenchymal tissue. Microfibril-associated protein 2 (*MFAP2*) plays a crucial role in cancer, notably promoting epithelial-mesenchymal transition (EMT). However, its involvement in OS remains unexplored.

**Methods:** *MFAP2* was silenced in U2OS cells using shRNA targeting *MFAP2* (sh-*MFAP2*) and validated by quantitative real-time polymerase chain reaction (qRT-PCR). We extracted gene chip data of *MFAP2* from multiple databases (GSE28424, GSE42572, and GSE126209). Correlation analyses between *MFAP2* and the Notch1 pathway identified through the gene set variation analysis (GSVA) enrichment analysis were conducted using the Pearson correlation method. Cellular behaviors (viability, migration, and invasion) were assessed via the Cell Counting Kit-8 (CCK-8), wound healing, and Transwell assays. EMT markers (N-cadherin, vimentin, and  $\beta$ -catenin) and Notch1 levels were examined by western blotting and qRT-PCR. Cell morphology was observed microscopically to evaluate EMT. Finally, the role of *MFAP2* in OS was validated through a xenograft tumor model.

**Results:** OS cell lines exhibited higher *MFAP2* mRNA expression than normal osteoblasts. *MFAP2* knockdown in U2OS cells significantly reduced viability, migration, and invasion, along with downregulation of N-cadherin and vimentin, as well as upregulation of  $\beta$ -catenin. *MFAP2* significantly correlated with the Notch1 pathway in OS and its knockdown inhibited Notch1 protein expression. Furthermore, Notch1 activation reversed the inhibitory effects of *MFAP2* knockdown on the malignant characteristic of U2OS cells. Additionally, *MFAP2* knockdown inhibited tumor growth, expression levels of EMT markers, and Notch1 expression in OS tumor tissues.

**Conclusions:** Our study revealed that *MFAP2* was an upstream regulator of the Notch1 signaling pathway to promote EMT in OS. These findings suggested *MFAP2* as a potential OS therapy target.

**Keywords:** Microfibril-associated protein 2 (MFAP2); epithelial mesenchymal transformation; osteosarcoma (OS); Notch1 pathway; neoplasm invasiveness

Submitted Nov 12, 2023. Accepted for publication Apr 17, 2024. Published online Jun 27, 2024.

doi: 10.21037/tcr-23-2035

**View this article at:** <https://dx.doi.org/10.21037/tcr-23-2035>

<sup>^</sup> ORCID: 0009-0003-0085-2449.

## Introduction

Osteosarcoma (OS), an exceptionally aggressive bone tumor, predominantly afflicts adolescents and young adults, comprising approximately 35% of all primary malignant bone tumors (1,2). The combination of neoadjuvant chemotherapy and advancements in surgical techniques has significantly increased overall survival rates, now approaching 70% (2). Despite treatment advances, the outlook for metastatic OS patients remains grim, highlighting the urgent need for a deeper understanding of the molecular mechanisms underlying its pathogenesis and progression (3).

Distant tumor cell metastasis continues to be a significant impediment to the effective treatment of OS patients (4). Epithelial-mesenchymal transition (EMT) is a pivotal biological process that participates in the initiation, progression, and metastasis of OS (5,6). This process leads to the loss of polarity and adhesive properties in epithelial cells, endowing them with migratory and invasive characteristics as they transform into mesenchymal-like cells (7). Capobianco *et al.* found that vitamin D can inhibit OS through EMT, suggesting the potential for targeting EMT to treat OS (8).

Microfibril-associated protein 2 (*MFAP2*) is a protein-coding gene located at 1p36.13 (9). It plays a significant role in influencing cell motility (10). Studies have shown that *MFAP2* promotes EMT in tumor cells, which are

involved in tumor invasion and metastasis, such as in liver cancer (11) and gastric cancer (12). Wang *et al.* highlighted that *MFAP2* contributed to facilitating the EMT process in gastric cancer (12). Additionally, Chen *et al.* discovered that silencing *MFAP2* resulted in heightened expression of the epithelial marker, E-cadherin, and decreased expression of the mesenchymal marker, vimentin, in B16 melanoma cells. This process implied that *MFAP2* promoted the development of EMT, which in turn regulated the migration and invasion of melanoma cells (13). However, whether *MFAP2* can promote the development of EMT in OS remains to be determined.

The protein product of the *MFAP2* gene, MAGP1 (14), has been demonstrated to bind to the Notch1 receptor, thereby activating signaling (15). Notch1 signaling is a highly conservative pathway that plays essential roles in cell fate determination and tissue development (16). Upon the binding of the Notch receptor to its corresponding ligand on the surface of neighboring cells, the intracellular domain is released from the cell membrane, translocated into the cell nucleus, and interacts with downstream molecules to regulate the Notch cascade (17). Research has demonstrated the significant involvement of the Notch1 pathway in the process of EMT (18). Activation of Notch1 signaling promotes EMT, which allows epithelial cells to acquire mesenchymal features and enhances their migratory and invasive abilities, thereby promoting tumor metastasis and invasion in breast cancer (18). Gao *et al.* demonstrated that *Notch1* promoted the malignant progression of OS through activation of the cell division cycle 20 (19). Nevertheless, it is currently uncertain whether *MFAP2* promotes EMT in OS by mediating the Notch1 pathway.

This study aimed to investigate the impact of *MFAP2* on EMT and its potential relationship with the Notch1 signaling in OS. Our findings may provide valuable insights into the complex regulatory network that drives OS progression and metastasis, ultimately contributing to the development of targeted therapies and improved clinical outcomes for OS patients. We present this article in accordance with the ARRIVE reporting checklist (available at <https://tc.amegroups.com/article/view/10.21037/tcr-23-2035/rc>).

## Methods

### Network pharmacology analysis

### Data collection and pre-processing

The gene chip data for OS, including GSE28424 (comprising 4 normal samples and 19 disease samples), GSE42572

### Highlight box

#### Key findings

- Microfibril-associated protein 2 (*MFAP2*) was an upstream regulator of the Notch1 signaling pathway to promote epithelial-mesenchymal transition (EMT) in osteosarcoma (OS) cells.

#### What is known and what is new?

- EMT is a pivotal biological process that participates in the initiation, progression, and metastasis of OS.
- The manuscript revealed that *MFAP2* induces EMT in OS by activating the Notch1 pathway.

#### What is the implication, and what should change now?

- The findings highlight the key player of *MFAP2* in EMT and its promotion of Notch1 signaling, providing valuable insights into the molecular mechanisms underlying OS progression. Targeting *MFAP2* may offer potential therapeutic strategies for inhibiting EMT and impeding OS tumor growth and metastasis.
- Given the manuscript's findings based on the *in vitro* experiments, additional studies should be conducted to further explore *in vivo* metastasis.

(comprising 5 normal samples and 7 disease samples), and GSE126209 (comprising 11 normal samples and 12 disease samples), were downloaded from the Gene Expression Omnibus (GEO) database (<https://www.ncbi.nlm.nih.gov/geo/>). Subsequently, gene annotation was performed for the probe sets based on the gene chip platform. Then, the data from all datasets were merged and batch effects were removed using the *sva* package in R software version 4.2.2. The study was conducted in accordance with the Declaration of Helsinki (as revised in 2013). A protocol was prepared before the study without registration.

### Validation of differential expression of *MFAP2* based on the merged dataset

Gene chip data for *MFAP2* were extracted from the merged dataset. The 'Wilcox. test' method was employed to assess its differential expression between the normal group and the OS group.

### Enrichment analysis of gene set variation analysis (GSVA)

Pathways related to *Notch1* were downloaded from the MSigDB database (20). Enrichment analysis was performed on previously merged datasets using the R software version 4.2.2 and the GSVA package to obtain activity scores of pathways in the samples. Subsequently, the *t*-test method was applied to identify differential pathways associated with OS. Finally, the Pearson correlation method was used to assess the correlation between the selected pathways and *MFAP2*.

### Cell culture

The human normal osteoblast cell line hFOB1.19 and OS cell lines HOS, U2OS, and MG63 were sourced from Wuhan Pricella Biotechnology Co., Ltd. (Wuhan, China). These cell lines were cultured in specific media: hFOB1.19 in DMEM/F12 (the 1:1 mixture of Dulbecco's Modified Eagle's Medium and Ham's F-12 Nutrient Mixture.), HOS in MEM, U2OS in DMEM, and MG63 in high-glucose DMEM (Gibco, CA, USA). The culture media were enriched with 10% fetal bovine serum (FBS) from Ephraim (Tianjin, China) and 1% double antibody from Hyclone (UT, USA). The cells were maintained in a 5% CO<sub>2</sub> incubator (Thermo Fisher Scientific, MA, USA) at 37 °C.

### Cell treatment and groups

After 4 h of starvation in the recommended growth

medium containing 1% FBS, U2OS cells were treated with 50 ng/mL of epidermal growth factor (EGF) for 30 min as the EFG group. Subsequently, the cells were transfected with lentiviral vectors for *MFAP2* knockdown and subjected to packaging for 48 h as EGF + shRNA targeting *MFAP2* (sh-MFAP2) group. The cells in the EGF + sh-NC (shRNA targeting negative control) group were transfected with sh-NC. U2OS cells stably transfected with sh-MFAP2 were treated for 24 h with the Notch1 activator valproic acid (VPA; 3 mM; YZ-1708707, Solarbio, Beijing, China) as the sh-MFAP2 + VPA group.

### Animals and diets

Twelve nude mice (BALB/c, 6 weeks old, weighing 18–20 g) were sourced from the Experimental Animal Center of Yangzhou University (Jiangsu, China). The mice were kept under controlled conditions, with a consistent temperature of 23 °C and a 12-h light/dark cycle. They had unrestricted access to both food and water. All animal-related procedures and experiments were conducted in strict accordance with institutional ethical standards and guidelines and were approved by the Ethical Committee for Animal Welfare at Yangzhou University (Approval No: 202308009).

### Tumor model construction

The mice were initially separated into two cohorts: the sh-NC group and the sh-MFAP2 group. After a one-week acclimation period, 4×10<sup>6</sup> U2OS cells, transfected with either sh-NC or sh-MFAP2, were introduced into the right axillary region of each mouse via subcutaneous injection (21,22). After 28 days, euthanasia was administered to the mice through the inhalation of 7.5% isoflurane, and the resulting tumors were collected. Detailed records and photographic documentation of the tumors were made, and they were subsequently preserved by fixation in a solution of 4% paraformaldehyde. The measurement of tumor volume was performed every 4 days, utilizing the formula: volume (mm<sup>3</sup>) = 1/2 × length × width<sup>2</sup>.

### Cell transfection

To achieve *MFAP2* knockdown, U2OS cells were subjected to transfection with specific shRNA oligonucleotide duplexes targeting *MFAP2* (shMFAP2), while a control sh-NC was also employed, and both were obtained from VectorBuilder Inc. (Guangzhou, China). When cellular

confluence reached between 70% to 90%, we proceeded with the gradual viral transduction using either sh-NC or sh-MFAP2. Following an 18-h transfection period, the culture medium was refreshed with a new complete culture medium. After 48 h of transfection, the culture medium was once again replaced, this time with a complete culture medium supplemented with 2.5 µg/mL puromycin, facilitating the selection of stably transfected cell lines. The efficiency of gene knockout was subsequently confirmed through quantitative real-time polymerase chain reaction (qRT-PCR).

### qRT-PCR

A qRT-PCR approach was employed to analyze changes in gene expression. First, following the experimental protocol of Amirouche *et al.* (23), adjustments were made to perform RNA extraction using the Trizol method. Subsequently, cDNA synthesis was performed using the FastKing gDNA Dispelling RT SuperMix kit (TIANGEN, Beijing, China) according to the manufacturer's instructions. For qRT-PCR reactions, SYBR Green PCR Master Mix (Lifeint, Xiamen, China) was utilized under the following conditions: an initial denaturation step at 95 °C for 30 s, followed by 40 cycles consisting of 5 s at 95 °C and 34 s at 60 °C. The relative gene expression was determined using the  $2^{-\Delta\Delta C_t}$  method, with *GAPDH* serving as the internal reference for normalization. Here are the primer sequences: *MFAP2* (human) forward primer: 5'-CTG ACC ACG TCC AGT ACA CC-3', reverse primer: 5'-TCC AGC TCT GCA TTT CCT GG-3'. *GAPDH* (human) forward primer: 5'-GGA GCG AGA TCC CTC CAA AAT-3', reverse primer: 5'-GGC TGT TGT CAT ACT TCT CAT GG-3'.

### Cell viability assays

Cell viability was assessed through the utilization of the Cell Counting Kit-8 (CCK-8) assay. Initially, 100 µL of cell suspension containing 2,000 cells per well was inoculated into a 96-well plate. This culture plate was then carefully placed within a 37°C incubator enriched with 5% CO<sub>2</sub> for pre-cultivation. Once the cells had achieved complete adherence, the transfection procedure was executed by the previously outlined steps. Following the transfection process, 10 µL of CCK-8 reaction solution sourced from Beyotime (Shanghai, China), was meticulously introduced into each well. Subsequently, the culture plate was incubated within a controlled environment for a period of 2 h. Upon

completion of the incubation, the absorbance of the samples was quantified at 450 nm utilizing a microplate reader (Wuxi Hiwell Diatek, Nanjing, China).

### Migration assays

Wound-healing assay was conducted to evaluate the migratory capacity of OS cells. First, horizontal lines were meticulously drawn at even intervals of approximately 0.5 cm on the underside of a 6-well plate, ensuring that each of the 6 wells was intersected by at least three lines. Subsequently, around  $5 \times 10^5$  U2OS cells were carefully introduced into each well, ensuring uniform coverage across the base. On the following day, the pipette tip was positioned as vertically as possible, aligned with a ruler over the previously drawn horizontal lines on the plate's underside, with a focus on maintaining a perpendicular orientation. Following these preparations, phosphate-buffered saline (PBS) was employed for a triple-round wash of the cell culture, with any dislodged cells being promptly removed. Subsequently, the serum-free culture medium was added to the wells. Sampling was carried out at 0 h, 24 h, and 48 h, during which images of the wound were meticulously captured using a microscope (Olympus, PA, USA). The formula was as follows: migration rate (%) =  $[1 - (\text{wound area at 24 h or 48 h} / \text{wound area at 0 h})] \times 100\%$ .

### Invasion assays

Matrigel was diluted 1:4 in culture medium to reach a final concentration of 50 mg/L to prepare the Matrigel coating. Then, we added 50 µL of this diluted Matrigel solution to the upper side of the Transwell chamber membrane and allowed it to solidify into a gel by incubating at 37 °C for 4 h. For cell seeding and invasion assays, we enzymatically detached the cells, washed them with PBS, and resuspended them in a serum-free culture medium to achieve a cell density of  $1 \times 10^5$  cells/mL. Then, we added 200 µL of this cell suspension to the upper chamber of the Transwell. In the lower chamber, we placed a culture medium containing 20% FBS. After 24 h of incubation at 37 °C in a CO<sub>2</sub> incubator for cell invasion, we removed the Transwell chambers. To assess invasion, we wiped off non-migrated cells from the upper side of the membrane with a cotton swab. We rinsed the chambers with PBS three times to remove any remaining non-migrated cells. Next, we fixed the chambers in ice-cold methanol for 30 min at 4 °C. After

air-drying, we stained the migrated cells with crystal violet for 20 min. The excess stain was washed off by rinsing the chambers with PBS three times. During the Transwell assay, imaging and cell counting were performed on three randomly selected fields of view using a microscope (Olympus).

### Western blotting

Cellular protein extraction was meticulously conducted using ice-cold radioimmunoprecipitation assay buffer (Beyotime). To ascertain the protein concentration, the highly regarded bicinchoninic acid (BCA) method from Beyotime was adeptly applied. Protein specimens were effectively separated utilizing precise 10% sodium dodecyl sulfate-polyacrylamide gel electrophoresis, after which they were judiciously transferred onto specialized 0.45  $\mu\text{m}$  polyvinylidene fluoride (PVDF) membranes (Beyotime). A comprehensive blocking process, employing 5% non-fat milk dissolved in TBST (Tris buffered saline with Tween 20), was meticulously carried out for a duration of 1 h at room temperature. Subsequently, these membranes underwent an incubation period of utmost precision, where they were allowed to interact with the corresponding primary antibodies at a constant temperature of 4 °C throughout the night. Following this crucial step, a secondary antibody was applied for a duration of 1 h. Finally, a mixture of equal volumes comprising the electrochemiluminescence detection reagents A and B (Applygen, Beijing, China) was expertly concocted. The PVDF membrane, after a meticulous 5-min wash, was delicately swathed with plastic wrap. After this, the membrane was artfully exposed to X-ray film (Servicebio, Wuhan, China) within the confines of a darkroom. The exposed film was subjected to scanning procedures and the resultant data was adeptly archived for subsequent analysis. To express the relative protein content, precise measurements of grayscale values of the protein bands were made, with particular attention given to comparing them against the grayscale values of internal reference protein bands. The specific primary antibodies employed in this study included GAPDH (1:1,000, #2118, CST, MA, USA),  $\beta$ -Catenin (1:1,000, #AF6266, Affinity, ON, CAN), N-Cadherin (1:1,000, #AF5239, Affinity), Vimentin (1:1,000, #AF7013, Affinity), and Notch1 (1:1,000, #3608, CST). For the secondary antibody, a Goat Anti-Rabbit IgG H&L (HRP; 1:2,000, #ab205718, Abcam, CB, UK) was judiciously employed.

### Statistical analysis

The data were expressed as the mean  $\pm$  standard deviation from three independent experiments. Statistical analysis was performed using one-way analysis of variance (ANOVA) followed by Tukey's post-hoc test to assess differences between groups. GraphPad 8.0 software was utilized for all statistical analyses, and  $P < 0.05$  denoted statistical significance.

## Results

### *MFAP2 promotes proliferation, migration, and invasion in OS cells*

To investigate the mechanism of *MFAP2* in OS, we first evaluated the expression of *MFAP2* in human normal osteoblasts hFOB1.19 and OS cell lines HOS, U2OS, and MG63. We observed significant *MFAP2* mRNA upregulation in OS cell lines in comparison with normal osteoblast cells ( $P < 0.01$ ). Notably, U2OS cells exhibited significantly higher *MFAP2* mRNA expression than HOS and MG63 cells ( $P < 0.01$ , *Figure 1A*). Then, we used sh-*MFAP2* to knock down its expression in U2OS cells. It was confirmed that *MFAP2* silenced at 48 h post-transfection relative to the sh-NC group transfected with an empty virus ( $P < 0.01$ ), demonstrating the successful construction of *MFAP2* knockdown in U2OS cells (*Figure 1B*). Subsequently, we detected the cell viability, migration, and invasion of U2OS cells. Cell migration and invasion are characteristics of tumor malignancy (24). As shown in *Figure 1C-1E*, our observations revealed that silencing *MFAP2* led to a marked reduction in cell viability, as well as decreased migration and invasion abilities in U2OS cells in comparison to the sh-NC group ( $P < 0.01$ ).

### *MFAP2 promotes EMT in OS cells*

The process of EMT is closely associated with the migration and invasion of tumor cells (24). N-cadherin, vimentin, and  $\beta$ -catenin are biomarkers of EMT (25,26). In contrast to the sh-NC group, the sh-*MFAP2* group demonstrated a notable decrease in the protein expression of N-cadherin and vimentin, while there was a marked increase in the protein expression of  $\beta$ -catenin ( $P < 0.01$ , *Figure 2A*). To further investigate the effect of *MFAP2* on EMT, we induced the U2OS cell lines with EGF, an EMT activator, and then observed cell morphology. As shown in *Figure 2B*, U2OS cells in the control group exhibited normal morphology,

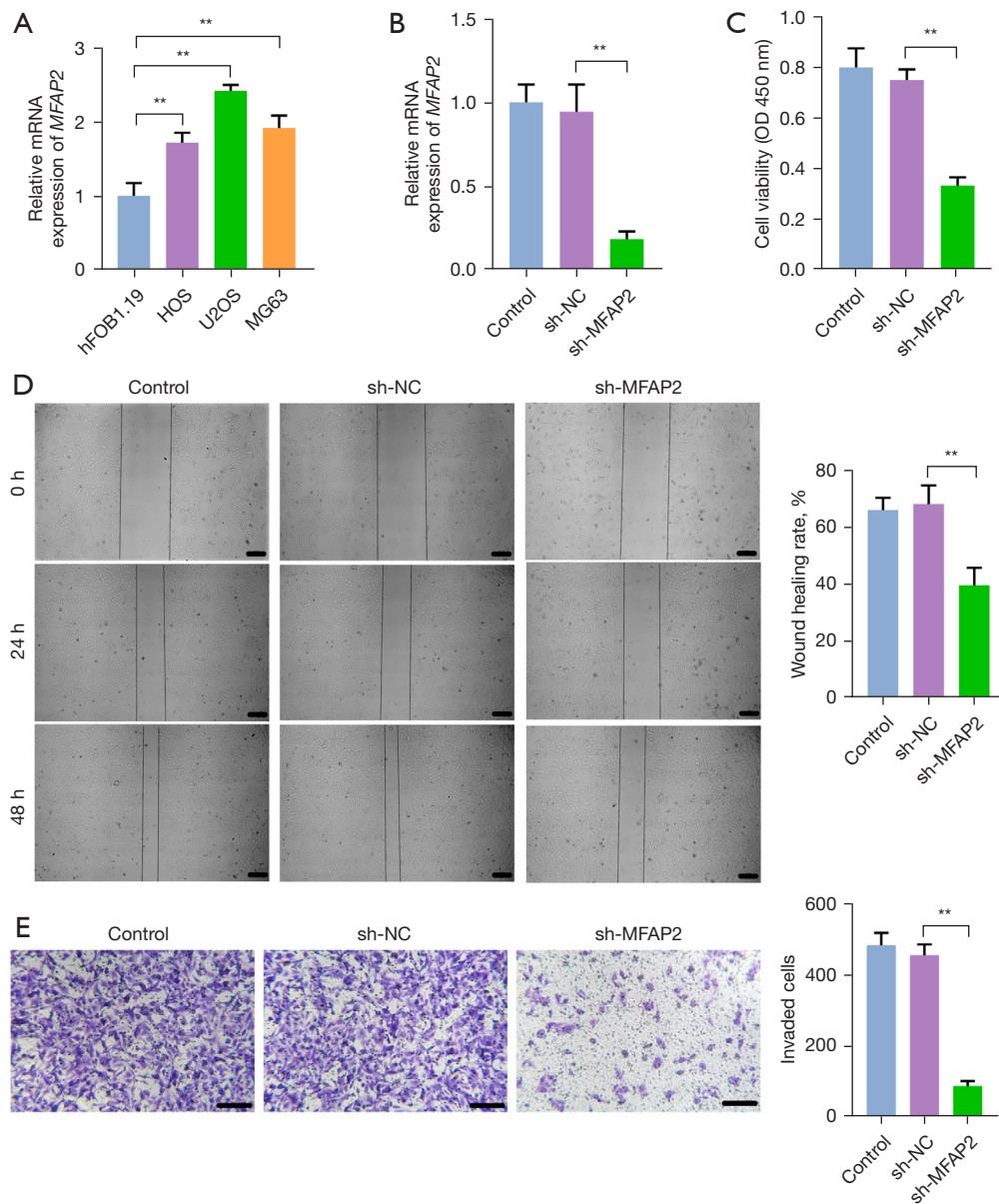


**Figure 1** MFAP2 promotes proliferation, migration, and invasion in OS cells. (A) The expression of MFAP2 in OS cell lines HOS, U2OS, MG63, and human normal osteoblast cell line HfoB1.19 was detected by qRT-PCR. (B) MFAP2 expression after sh-MFAP2 or sh-NC transfection in U2OS cells. (C) Cell viability of U2OS cells was detected by CCK-8 assay. (D) The cell migration capability of U2OS cells was detected by wound healing assay and observed under a microscope; scale bar =150  $\mu$ m. (E) The cell invasive capability of U2OS cells was detected by Transwell and observed under a microscope; scale bar =150  $\mu$ m. U2OS cells were cultured in DMEM medium containing 10% FBS and 1% antibiotics at 37  $^{\circ}$ C with 5% CO<sub>2</sub> in a humidified environment, and were transfected with either sh-NC or sh-MFAP2. \*\*, P<0.01. sh-NC, shRNA targeting negative control; OD, optical density; MFAP2, microfibril-associated protein 2; OS, osteosarcoma; qRT-PCR, quantitative real-time polymerase chain reaction; CCK-8, Cell Counting Kit-8; DMEM, Dulbecco's modified Eagle medium; FBS, fetal bovine serum.

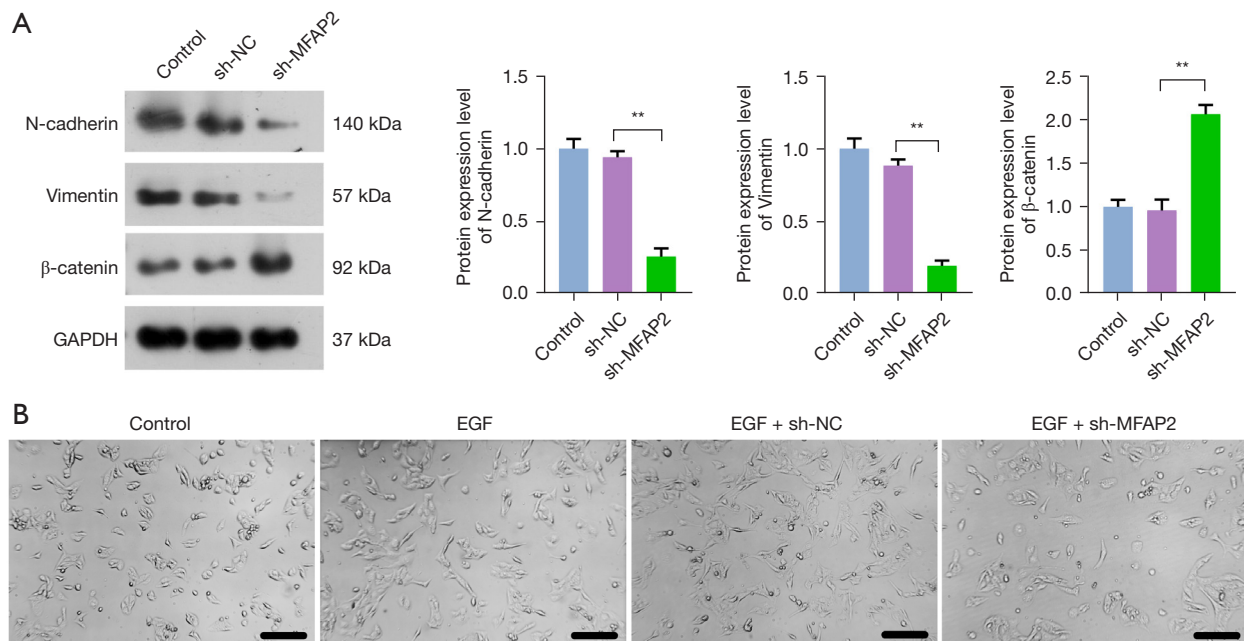


**Figure 2** *MEAP2* promotes EMT in OS cells. (A) Western blotting detected the protein levels of EMT markers (N-cadherin, vimentin, and  $\beta$ -catenin) in U2OS cells. (B) EGF-induced morphological change of U2OS cells using a microscope; scale bar = 150  $\mu$ m. U2OS cells were treated with EGF and/or transfected with sh-NC or sh-MFAP2. \*\*,  $P < 0.01$ . sh-NC, shRNA targeting negative control; MFAP2, microfibril-associated protein 2; GAPDH, glyceraldehyde-3-phosphate dehydrogenase; EMT, epithelial-mesenchymal transition; OS, osteosarcoma; EGF, epidermal growth factor.

while they transformed into elongated fibroblast-like shapes after EGF treatment. In comparison to the EGF + sh-NC group, inhibition of *MEAP2* resulted in EGF-induced U2OS cells exhibiting morphology closer to the normal state.

#### *MEAP2 is significantly correlated with Notch1 pathway*

Using the *sva* package in R software version 4.2.2, we merged and removed batch effects from the gene chip data in datasets (GSE28424, GSE42572, and GSE126209). The resulting dataset was designated as Dataset 1, and the integration of data showed promising results (Figure S1). Subsequently, we examined the differential expression of the *MEAP2* between the normal and OS groups in Dataset 1. The expression level of *MEAP2* was notably higher in the OS group compared to the normal group, as illustrated in Figure 3A ( $P < 0.05$ ). To explore the association between *MEAP2* and the Notch1 pathway, we initially retrieved five pathways from the MsigDB database. Following GSVA enrichment analysis and *t*-test, we identified three pathways with significant differences between the OS and

normal groups. These pathways were Reactome\_signaling by Notch1, Kyoto Encyclopedia of Genes and Genomes (KEGG)\_Notch signaling pathway, and WikiPathways (WP)\_Notch signaling. As illustrated in Figure 3B, the activity scores of these three pathways were significantly higher in the OS group than in the normal group ( $P < 0.05$ ). For the selected pathways, we conducted correlation analysis with *MEAP2* using the Pearson correlation method. The analysis results demonstrated a significant positive correlation between *MEAP2* and the Reactome signaling by the Notch1 pathway as well as the KEGG Notch signaling pathway (Figure 3C,  $P < 0.05$ ).

#### *MEAP2 promotes EMT in OS cells by activating the Notch1 pathway*

*MEAP2* can bind to the Notch1 receptor, thereby initiating signal transduction pathways (27). This activation of the Notch1 signaling pathway can facilitate the onset of EMT, consequently enhancing tumor metastasis and invasion (28). To investigate whether *MEAP2* promotes EMT in OS cells through the activation of the Notch1

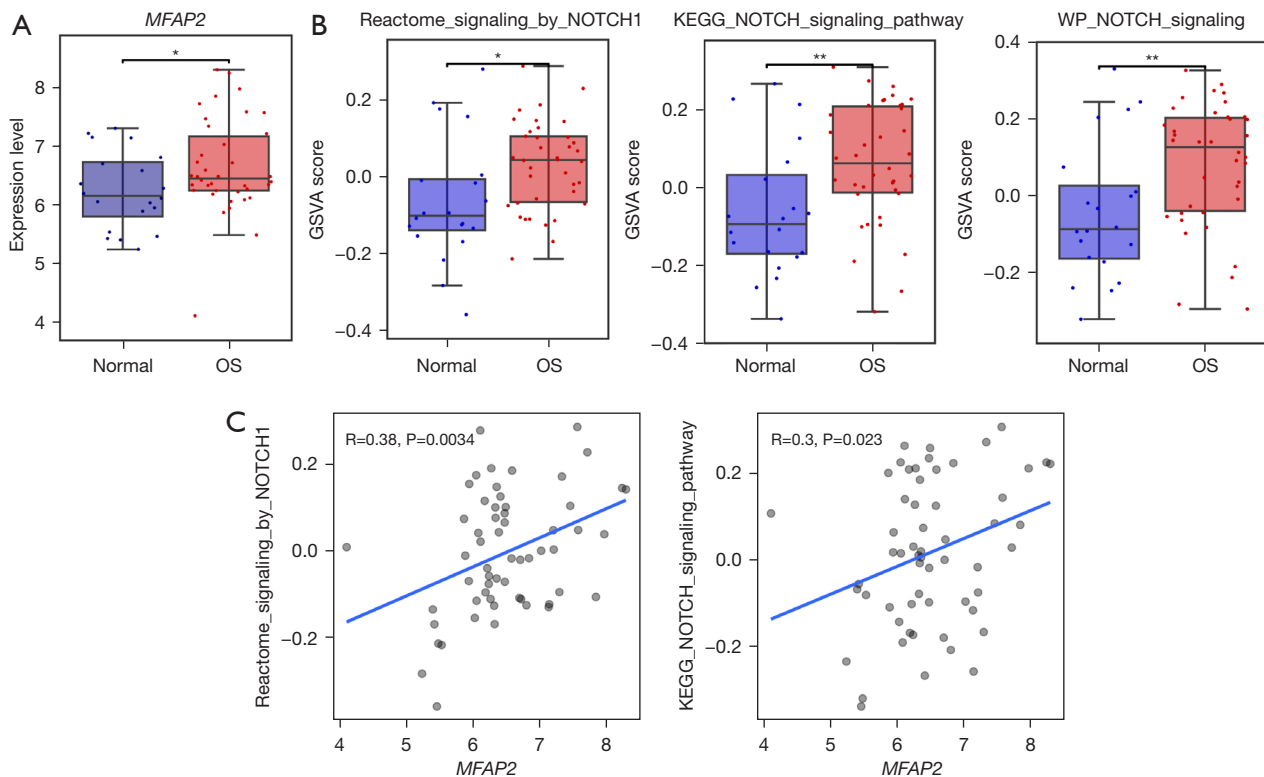


**Figure 3** *MFAP2* is significantly correlated with the Notch1 pathway. (A) Expression distribution of *MFAP2* in the normal and OS groups. (B) GSVAscores of three pathways (Reactome\_signaling by Notch1, KEGG\_Notch signaling pathway, and WP\_Notch signaling) in the normal and OS groups. (C) Scatter plot of correlation between *MFAP2* and Reactome\_signaling by Notch1, and KEGG\_Notch signaling pathway. \*,  $P < 0.05$ ; \*\*,  $P < 0.01$ . *MFAP2*, microfibril-associated protein 2; OS, osteosarcoma; GSVAs, gene set variation analysis; KEGG, Kyoto Encyclopedia of Genes and Genomes; WP, WikiPathways.

pathway, we knocked down *MFAP2* in OS cells and then treated with VPA (a Notch1 activator). As shown in *Figure 4A*, in contrast to the sh-NC group, there was a significant reduction in Notch1 protein expression within the sh-*MFAP2* group ( $P < 0.05$ ). Nevertheless, the introduction of VPA effectively counteracted the inhibitory impact of *MFAP2* knockdown on Notch1 protein expression. These findings affirmed that *MFAP2* actively triggered the Notch1 pathway in OS. Subsequently, we proceeded to evaluate the effects on OS cell viability and invasion. The results unveiled that VPA robustly reversed the inhibitory consequences of *MFAP2* knockdown on the malignant traits of OS cells. Furthermore, VPA effectively annulled the suppressive influence of *MFAP2* knockdown on EMT biomarker levels, leading to a marked increase in the expression of N-cadherin, vimentin, and  $\beta$ -catenin in OS cells ( $P < 0.01$ , *Figure 4B-4D*). Together, these results provided sufficient evidence that *MFAP2* promoted EMT

in OS cells through activation of the Notch1 pathway.

#### **Validation of the promotional effect of *MFAP2* on OS progression in xenograft tumor model mice**

We also assessed the influence of *MFAP2* on tumor growth in the mouse model. Notably, there was a substantial reduction in both tumor volume and weight following *MFAP2* knockdown compared to the sh-NC group ( $P < 0.01$ , *Figure 5A, 5B*). Furthermore, we analyzed the mRNA expression profiles of EMT biomarkers within the OS tumor tissues. Intriguingly, in the sh-*MFAP2* group, there was a significant reduction in the expression levels of N-cadherin and vimentin when compared to the sh-NC group ( $P < 0.01$ , *Figure 5C*), indicating that inhibiting *MFAP2* effectively suppressed the EMT process in OS tumor tissues. Furthermore, western blot analysis results indicated that the Notch1 signaling pathway was markedly



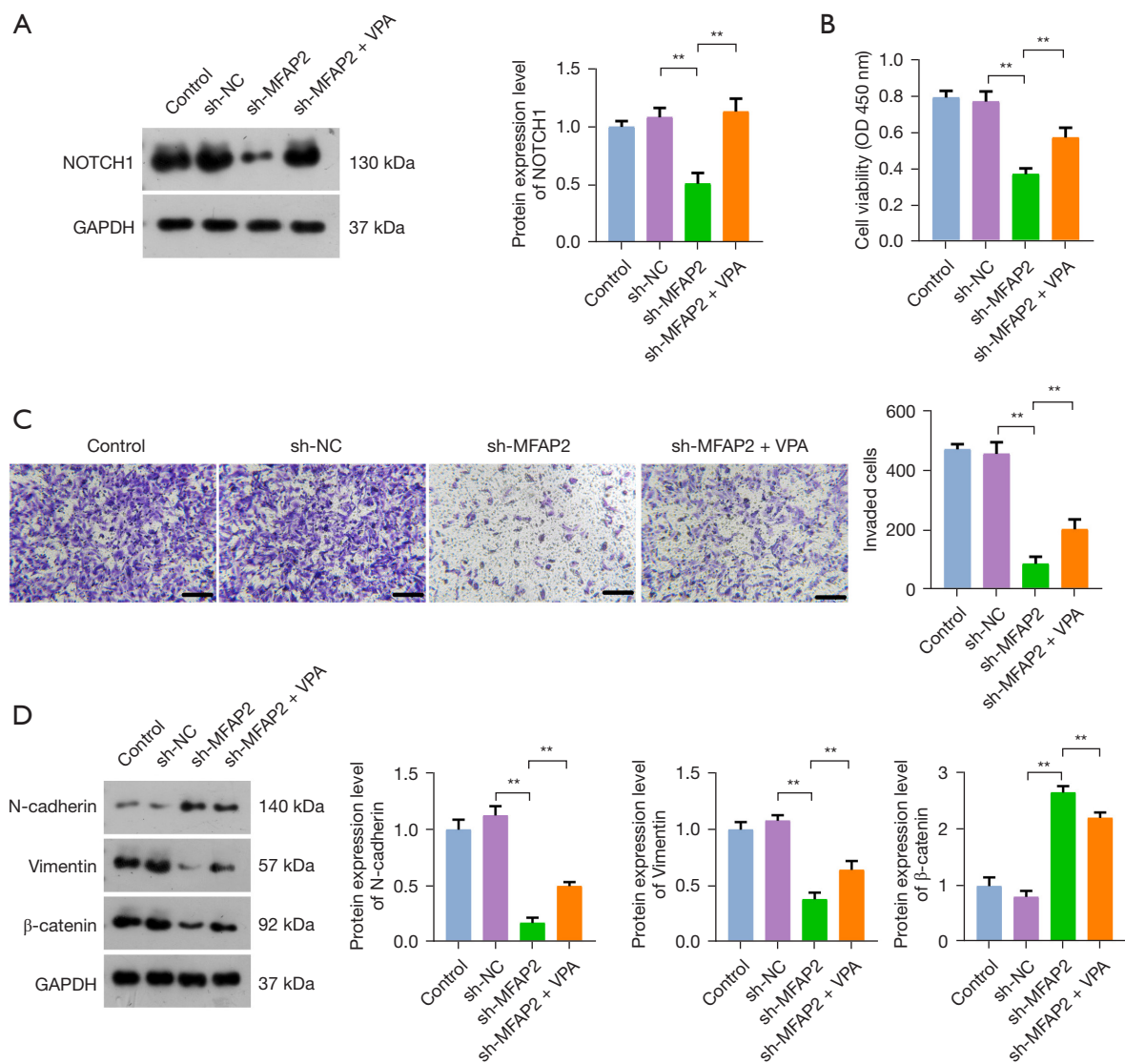


**Figure 4** *MEAP2* promotes EMT in OS cells through activation of the Notch1 pathway. (A) Western blotting examined the protein levels of Notch1 in *MEAP2*-knockdown U2OS cells treated with VPA. (B) Cell viability of U2OS cells was assessed using the CCK-8 assay. (C) Cell invasion ability of U2OS cells was assessed by Transwell invasion assay and observed under a microscope; scale bar =150  $\mu$ m. (D) Western blotting analyses of the protein levels of EMT markers (N-cadherin, vimentin, and  $\beta$ -catenin) in U2OS cells. U2OS cells were transfected with sh-MFAP2 and treated with 3 mmol/L VPA (a Notch1 activator) for 24 h. \*\*,  $P < 0.01$ . sh-NC, shRNA targeting negative control; MFAP2, microfibril-associated protein 2; GAPDH, glyceraldehyde-3-phosphate dehydrogenase; EMT, epithelial-mesenchymal transition; OS, osteosarcoma; CCK-8, Cell Counting Kit-8; VPA, valproic acid.

inhibited in the sh-MFAP2 group ( $P < 0.01$ , Figure 5D).

## Discussion

The present study demonstrated that *MEAP2* induced EMT in OS by activating the Notch1 signaling pathway. First, the significant correlation between *MEAP2* and

the Notch1 signaling pathway in OS was validated. In addition, our investigation revealed an upregulation of *MEAP2* expression in OS. The establishment of stable *MEAP2* knockdown led to a noteworthy inhibition in OS cell proliferation, migration, invasion, and the progression of EMT. Furthermore, the activation of Notch1 effectively counteracted the inhibitory effects of *MEAP2* knockdown

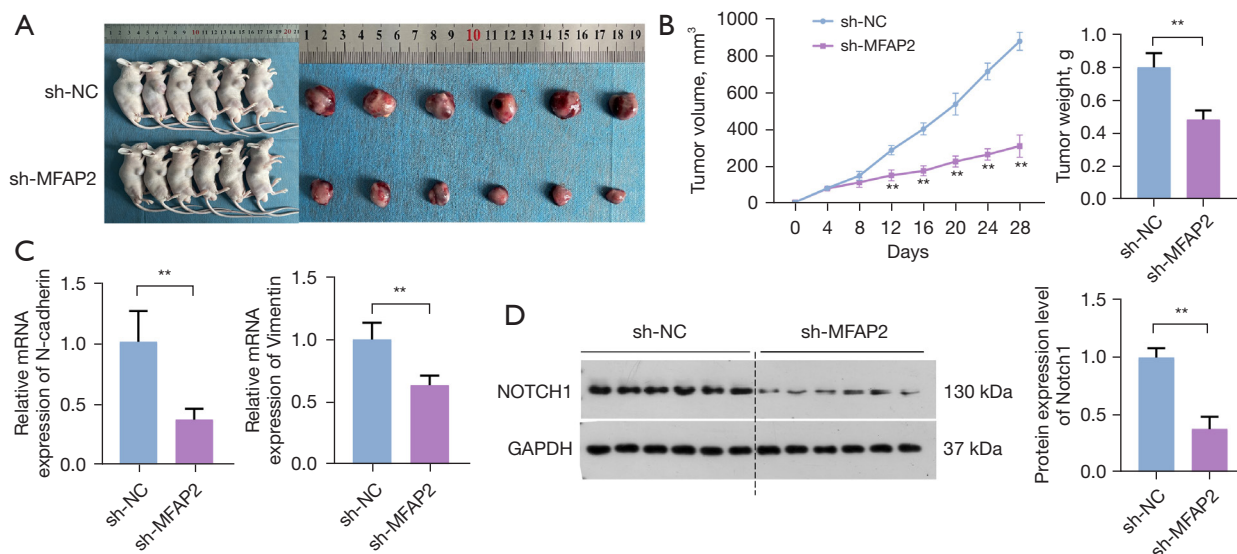


**Figure 5** Validation of the promotional effect of *MFAP2* on OS progression using animal experiments. (A) Tumor growth. (B) Tumor volume and tumor weight. (C) The mRNA expression of N-cadherin and vimentin in tumor tissue of model mice. (D) The protein expression of Notch1 in tumor tissue of model mice. The OS model was established by injecting nude mice with U2OS cells transfected with  $4 \times 10^6$  sh-NC or sh-MFAP2. \*\*,  $P < 0.01$ . sh-NC, shRNA targeting negative control; MFAP2, microfibril-associated protein 2; GAPDH, glyceraldehyde-3-phosphate dehydrogenase; OS, osteosarcoma.

on the malignant behavior of OS cells. Finally, the role of *MFAP2* in inducing EMT in OS and its potential relationship with Notch1 activation were verified in a xenograft tumor mice model.

The induction of EMT plays a crucial role in the spread and transfer of malignant cells during the progression of OS (29). The process of tumor EMT encompasses the transformation of epithelial cells into a mesenchymal, fibroblast-like phenotype, resulting in enhanced cellular motility and migratory capacity (30). This transition involves the reduction in the expression of epithelial cell markers such as  $\beta$ -catenin and E-cadherin, accompanied by the concurrent increase in the expression of mesenchymal cell markers, including N-cadherin, vimentin, and fibronectin (4,31). Prior research has provided evidence of *MFAP2*'s involvement in the regulation of EMT across various cancer types (12). Dong *et al.* found that there was an elevation in E-cadherin expression while reduction in vimentin, N-cadherin, and  $\beta$ -catenin after suppressing *MFAP2* expression in papillary thyroid carcinoma cells (9). As part of this analysis, *MFAP2* knockdown reduced cell viability, migration, and invasion capability of U2OS cells and OS tumor size in mice. Importantly, our results demonstrated that *MFAP2* knockdown effectively

upregulated the levels of  $\beta$ -catenin and downregulated the levels of N-cadherin and vimentin in U2OS cells as well as OS tumor tissues. The differences in  $\beta$ -catenin expression might be associated with the characteristics of the tumor and the status of its internal signaling pathways. Moreover, EGF is an important inducer of EMT (32). In our study, *MFAP2* knockdown U2OS cell lines treated with EGF exhibited morphology closer to the normal state, suggesting that *MFAP2* knockdown inhibited the activation of EMT. Thus, these results demonstrated that *MFAP2* inhibition restressed malignant features, especially EMT, in OS.

The interaction between *MFAP2* and Notch1 results in the release of the extracellular domain of Notch1, subsequently activating Notch signaling (15). The impact of *MFAP2* on Notch signaling holds significance in cancer (33). In our study, *MFAP2* exhibited a significant correlation with the Notch1 signaling pathway in OS. Furthermore, *MFAP2* knockdown led to a reduction in Notch1 expression of OS tumor tissues. Taken together, these findings suggested that *MFAP2* functioned upstream of the Notch signaling in U2OS cells. Additionally, Notch1 signaling is a key driver for EMT activation (34). Besides, Zhang *et al.* proved that the Notch1 signaling pathway plays a crucial role in OS (35). He *et al.* also found that the suppression of Notch1 signaling led

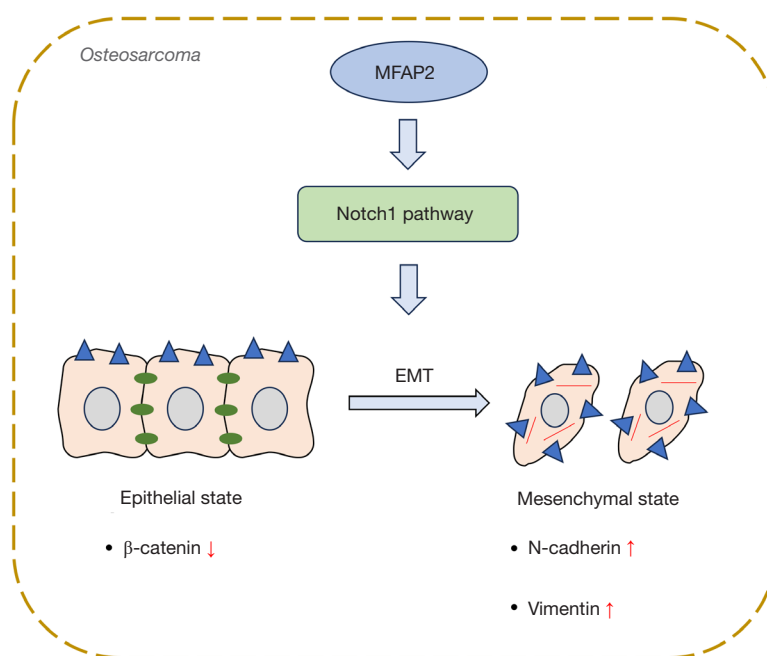


**Figure 6** A flow diagram illustrating the putative molecular mechanism by which MFAP2 induces EMT in OS cells through activation of the Notch1 pathway. MFAP2, microfibril-associated protein 2; EMT, epithelial-mesenchymal transition; OS, osteosarcoma.

to a decrease in cell proliferation and an enhancement in the osteogenic differentiation of bone marrow mesenchymal stem cells (17). Moreover, Gao *et al.* concluded that inhibition of *Notch1* suppressed cell viability, migration, and invasive capability of OS cells, thereby inhibiting the malignant development of OS (19). These findings aligned with our results. We observed that the Notch1 activator reversed the inhibition effects of *MFAP2* knockdown on cell viability, invasion, and EMT in U2OS cells. These results supported the role of *MFAP2* in promoting the EMT of OS cells by activating the Notch1 pathway.

Despite the significant progress made in this study, further investigations are required to identify potential crosstalk with other signaling pathways involved in EMT regulation. Moreover, current research is primarily focused on cellular and mouse models, and the translation to clinical applications still requires further research for validation and confirmation.

## Conclusions

Our research demonstrates that *MFAP2* induces EMT in OS cells by activating the Notch1 pathway (Figure 6). Our findings indicated a significant upregulation of *MFAP2* in both OS cells and tumor tissues. *MFAP2* knockdown

inhibited OS tumor growth, malignant characteristics, and EMT progress. Notch1 activation reversed the inhibition of *MFAP2* knockdown on OS progression and EMT. The identification of *MFAP2* as a key player in EMT and its promotion of Notch1 signaling provides valuable insights into the molecular mechanisms underlying OS progression. Targeting *MFAP2* may offer potential therapeutic strategies for inhibiting EMT and impeding OS tumor growth and metastasis. However, we initially demonstrated the promotion of EMT by *MFAP2* through the assessment of EMT-related markers (N-cadherin and vimentin) in *in vitro* experiments. Additional studies will be conducted to further explore *in vivo* metastasis.

## Acknowledgments

**Funding:** This work was supported by The Cultivating Scientific Research Project of the Second Hospital of Dalian Medical University (No. dy2yynpy202219). The authors expressed gratitude to Yangzhou University for providing us with the experimental platform.

## Footnote

**Reporting Checklist:** The authors have completed the

ARRIVE reporting checklist. Available at <https://tcr.amegroups.com/article/view/10.21037/tcr-23-2035/rc>

*Data Sharing Statement:* Available at <https://tcr.amegroups.com/article/view/10.21037/tcr-23-2035/dss>

*Peer Review File:* Available at <https://tcr.amegroups.com/article/view/10.21037/tcr-23-2035/prf>

*Conflicts of Interest:* All authors have completed the ICMJE uniform disclosure form (available at <https://tcr.amegroups.com/article/view/10.21037/tcr-23-2035/coif>). The authors have no conflicts of interest to declare.

*Ethical Statement:* The authors are accountable for all aspects of the work in ensuring that questions related to the accuracy or integrity of any part of the work are appropriately investigated and resolved. The study was conducted in accordance with the Declaration of Helsinki (as revised in 2013). All animal-related procedures and experiments were conducted in strict accordance with institutional ethical standards and guidelines and were approved by the Ethical Committee for Animal Welfare at Yangzhou University (Approval No: 202308009).

*Open Access Statement:* This is an Open Access article distributed in accordance with the Creative Commons Attribution-NonCommercial-NoDerivs 4.0 International License (CC BY-NC-ND 4.0), which permits the non-commercial replication and distribution of the article with the strict proviso that no changes or edits are made and the original work is properly cited (including links to both the formal publication through the relevant DOI and the license). See: <https://creativecommons.org/licenses/by-nc-nd/4.0/>.

## References

1. Zhao X, Wu Q, Gong X, et al. Osteosarcoma: a review of current and future therapeutic approaches. *Biomed Eng Online* 2021;20:24.
2. Jiang Y, Wang J, Sun M, et al. Multi-omics analysis identifies osteosarcoma subtypes with distinct prognosis indicating stratified treatment. *Nat Commun* 2022;13:7207.
3. Sheng G, Gao Y, Yang Y, et al. Osteosarcoma and Metastasis. *Front Oncol* 2021;11:780264.
4. Shao S, Piao L, Wang J, et al. Tspan9 Induces EMT and Promotes Osteosarcoma Metastasis via Activating FAK-Ras-ERK1/2 Pathway. *Front Oncol* 2022;12:774988.
5. Yang J, Antin P, Berx G, et al. Guidelines and definitions for research on epithelial-mesenchymal transition. *Nat Rev Mol Cell Biol* 2020;21:341-52.
6. Yu X, Yustein JT, Xu J. Research models and mesenchymal/epithelial plasticity of osteosarcoma. *Cell Biosci* 2021;11:94.
7. Kim H, Lee S, Shin E, et al. The Emerging Roles of Exosomes as EMT Regulators in Cancer. *Cells* 2020;9:861.
8. Capobianco E, McGaughey V, Seraphin G, et al. Vitamin D inhibits osteosarcoma by reprogramming nonsense-mediated RNA decay and SNAI2-mediated epithelial-to-mesenchymal transition. *Front Oncol* 2023;13:1188641.
9. Dong SY, Chen H, Lin LZ, et al. MFAP2 is a Potential Diagnostic and Prognostic Biomarker That Correlates with the Progression of Papillary Thyroid Cancer. *Cancer Manag Res* 2020;12:12557-67.
10. Yao LW, Wu LL, Zhang LH, et al. MFAP2 is overexpressed in gastric cancer and promotes motility via the MFAP2/integrin  $\alpha 5\beta 1$ /FAK/ERK pathway. *Oncogenesis* 2020;9:17.
11. Xu W, Wang M, Bai Y, et al. The role of microfibrillar-associated protein 2 in cancer. *Front Oncol* 2022;12:1002036.
12. Wang JK, Wang WJ, Cai HY, et al. MFAP2 promotes epithelial-mesenchymal transition in gastric cancer cells by activating TGF- $\beta$ /SMAD2/3 signaling pathway. *Onco Targets Ther* 2018;11:4001-17.
13. Chen Z, Lv Y, Cao D, et al. Microfibril-Associated Protein 2 (MFAP2) Potentiates Invasion and Migration of Melanoma by EMT and Wnt/ $\beta$ -Catenin Pathway. *Med Sci Monit* 2020;26:e923808.
14. Combs MD, Knutsen RH, Broekelmann TJ, et al. Microfibril-associated glycoprotein 2 (MAGP2) loss of function has pleiotropic effects in vivo. *J Biol Chem* 2013;288:28869-80.
15. Miyamoto A, Lau R, Hein PW, et al. Microfibrillar proteins MAGP-1 and MAGP-2 induce Notch1 extracellular domain dissociation and receptor activation. *J Biol Chem* 2006;281:10089-97.
16. Zhou B, Lin W, Long Y, et al. Notch signaling pathway: architecture, disease, and therapeutics. *Signal Transduct Target Ther* 2022;7:95.
17. He Y, Zou L. Notch-1 inhibition reduces proliferation and promotes osteogenic differentiation of bone marrow mesenchymal stem cells. *Exp Ther Med* 2019;18:1884-90.
18. Miao K, Lei JH, Valecha MV, et al. NOTCH1 activation compensates BRCA1 deficiency and promotes triple-

- negative breast cancer formation. *Nat Commun* 2020;11:3256.
19. Gao Y, Bai L, Shang G. Notch-1 promotes the malignant progression of osteosarcoma through the activation of cell division cycle 20. *Aging (Albany NY)* 2020;13:2668-80.
  20. Liberzon A, Birger C, Thorvaldsdóttir H, et al. The Molecular Signatures Database (MSigDB) hallmark gene set collection. *Cell Syst* 2015;1:417-25.
  21. Liu Y, She W, Li Y, et al. Aa-Z2 triggers ROS-induced apoptosis of osteosarcoma by targeting PDK-1. *J Transl Med* 2023;21:7.
  22. Sun X, Zhao X, Xu S, et al. CircSRSF4 Enhances Proliferation, Invasion, and Migration to Promote the Progression of Osteosarcoma via Rac1. *Int J Mol Sci* 2022;23:6200.
  23. Amirouche A, Ait-Ali D, Nouri H, et al. TRIzol-based RNA extraction for detection protocol for SARS-CoV-2 of coronavirus disease 2019. *New Microbes New Infect* 2021;41:100874.
  24. Liu W, Xin M, Li Q, et al. IL-17A Promotes the Migration, Invasion and the EMT Process of Lung Cancer Accompanied by NLRP3 Activation. *Biomed Res Int* 2022;2022:7841279.
  25. Zhu GJ, Song PP, Zhou H, et al. Role of epithelial-mesenchymal transition markers E-cadherin, N-cadherin,  $\beta$ -catenin and ZEB2 in laryngeal squamous cell carcinoma. *Oncol Lett* 2018;15:3472-81.
  26. Chaw SY, Abdul Majeed A, Dalley AJ, et al. Epithelial to mesenchymal transition (EMT) biomarkers--E-cadherin, beta-catenin, APC and Vimentin--in oral squamous cell carcinogenesis and transformation. *Oral Oncol* 2012;48:997-1006.
  27. Haider C, Hnat J, Wagner R, et al. Transforming Growth Factor- $\beta$  and Axl Induce CXCL5 and Neutrophil Recruitment in Hepatocellular Carcinoma. *Hepatology* 2019;69:222-36.
  28. Qian XQ, Tang SS, Shen YM, et al. Notch1 Affects Chemo-resistance Through Regulating Epithelial-Mesenchymal Transition (EMT) in Epithelial Ovarian cancer cells. *Int J Med Sci* 2020;17:1215-23.
  29. Cao Y, Chen E, Wang X, et al. An emerging master inducer and regulator for epithelial-mesenchymal transition and tumor metastasis: extracellular and intracellular ATP and its molecular functions and therapeutic potential. *Cancer Cell Int* 2023;23:20.
  30. Dongre A, Weinberg RA. New insights into the mechanisms of epithelial-mesenchymal transition and implications for cancer. *Nat Rev Mol Cell Biol* 2019;20:69-84.
  31. Loh CY, Chai JY, Tang TF, et al. The E-Cadherin and N-Cadherin Switch in Epithelial-to-Mesenchymal Transition: Signaling, Therapeutic Implications, and Challenges. *Cells* 2019;8:1118.
  32. Liu P, Yang P, Zhang Z, et al. Ezrin/NF- $\kappa$ B Pathway Regulates EGF-induced Epithelial-Mesenchymal Transition (EMT), Metastasis, and Progression of Osteosarcoma. *Med Sci Monit* 2018;24:2098-108.
  33. Craft CS, Broekelmann TJ, Mecham RP. Microfibril-associated glycoproteins MAGP-1 and MAGP-2 in disease. *Matrix Biol* 2018;71-72:100-11.
  34. Shao S, Zhao X, Zhang X, et al. Notch1 signaling regulates the epithelial-mesenchymal transition and invasion of breast cancer in a Slug-dependent manner. *Mol Cancer* 2015;14:28.
  35. Zhang K, Wu S, Wu H, et al. Effect of the Notch1-mediated PI3K-Akt-mTOR pathway in human osteosarcoma. *Aging (Albany NY)* 2021;13:21090-101.

**Cite this article as:** Jiang S, Zheng Z, Yuan B, Yan R, Yao Q, Chen H, Zhang Y, Lei Y, Liang H. MFAP2 induces epithelial-mesenchymal transformation of osteosarcoma cells by activating the Notch1 pathway. *Transl Cancer Res* 2024;13(6):2847-2859. doi: 10.21037/tcr-23-2035